Available online at www.sciencedirect.com
SCIENCE DIRECT®
Physica A 362 (2006) 42–47
PHYSICA A
www.elsevier.com/locate/physa

Simulations of complex fluids by mixed lattice Boltzmann—finite difference methods

Aiguo Xu[a,b,c,1], G. Gonnella[a,b,c], A. Lamura[d,*]

[a]Dipartimento di Fisica, Università di Bari, Italy
[b]TIRES, Center of Innovative Technologies for Signal Detection and Processing, Italy
[c]INFN, Sezione di Bari, Via Amendola 173, 70126 Bari, Italy
[d]Istituto Applicazioni Calcolo, CNR, Sezione di Bari, Via Amendola 122/D, 70126 Bari, Italy

Available online 4 October 2005

Abstract

We present the numerical results of simulations of complex fluids under shear flow. We employ a mixed approach which combines the lattice Boltzmann method for solving the Navier–Stokes equation and a finite difference scheme for the convection–diffusion equation. The evolution in time of shear banding phenomenon is studied. This is allowed by the presented numerical model which takes into account the evolution of local structures and their effect on fluid flow.

Keywords: Lattice Boltzmann method; Finite difference equation; Lamellar phase

1. Introduction

Complex fluids are characterized by the presence of organized structures at mesoscopic scales located between the molecular and the sample size. For example, di-block copolymer systems, consisting of solutions of A-polymers and B-polymers covalently bonded end-to-end in pairs, can organize in striped phases where A-rich regions are separated from B-rich regions by lamellae [1].

The interplay occurring in complex fluids between mesoscopic structures (interfaces, colloidal particles, etc.) and the local velocity field is particularly relevant. In presence of applied shear flows new structures or textures can be created not existing at rest. Such shear-induced structures (SIS) can coexist in some range of shear rate $\dot{\gamma}$ with the structures unmodified by the flow. Usually the SIS and the unmodified phase have different viscosities so that they flow with different velocity profiles. This phenomenon, called shear banding, has been observed in many complex fluids and also in lamellar systems [2].

Simulations at mesoscopic scales can be very useful for understanding the dynamics of complex fluids. In experiments it is often possible only to measure averaged velocity profiles or other quantities while the knowledge of the local behaviour of structures and flow gives essential information on the kinetics of

*Corresponding author. Tel.: +39 0805929745; fax: +39 0805929770.
E-mail address: a.lamura@ba.iac.cnr.it (A. Lamura).
[1]Present address: Division of Physics and Astronomy, Yoshida-south Campus, Kyoto University, Kyoto 606-8501, Japan.

0378-4371/$ - see front matter
doi:10.1016/j.physa.2005.09.015

formation of SIS, on the interface between the two bands, etc. On the other hand, models based on constitutive equations [1] cannot provide direct information on local structures in the fluid.

For these reasons, we present in this paper a generalization of lattice Boltzmann methods (LBM) useful for simulating complex fluids with dynamics described by Navier–Stokes and convection–diffusion equations [3]. We show how our method can be used for studying shear banding phenomena in systems with a lamellar phase. Our method uses LBM approach for the Navier–Stokes equation [4] and finite difference schemes for the convection–diffusion equation [5]. The approach to equilibrium is guaranteed by the choice of a free energy to calculate the pressure tensor and the chemical potential, appearing respectively in the Navier–Stokes and in the convection–diffusion equation [6].

An advantage of the mixed approach is that the continuum limit of the convection–diffusion equation can be better controlled and the required memory can be reduced for about a 50% factor. The numerical method will be described with details in Section 2. In Section 3 we show and discuss the results obtained in simulations with a shear flow acting on the system.

2. The model

The equilibrium phase is described by a coarse grained free energy. For the specific problem that we study here we use the following:

$$F = \int \mathrm{d}\mathbf{r}\left[\frac{1}{3}n\ln n + \frac{a}{2}\varphi^2 + \frac{b}{4}\varphi^4 + \frac{\kappa}{2}(\nabla\varphi)^2 + \frac{d}{2}(\nabla^2\varphi)^2\right], \tag{1}$$

where n is the total density of the mixture and φ is a scalar order parameter representing the concentration difference between the two components of the mixture. The term in n gives rise to a positive background pressure and does not affect the phase behaviour. The terms in φ correspond to the Brazovskii free energy [7]. We take $b, d > 0$ to ensure stability. For $a > 0$ the fluid is disordered; for $a < 0$ it prefers an ordered state whose nature depends on the value of κ. Indeed, for negative values of κ there is a transition when $b = -a$ into a lamellar state with characteristic wave-vector $q = \sqrt{-\kappa/2d}$.

The evolution of φ is described by a convection–diffusion equation which ensures its conservation and allows to couple it with the fluid motion:

$$\partial_t\varphi + \boldsymbol{\nabla}\cdot(\varphi\mathbf{u}) = \Gamma\nabla^2\mu, \tag{2}$$

where

$$\mu = \frac{\delta F}{\delta\varphi} = a\varphi + b\varphi^3 - \kappa\nabla^2\varphi + d(\nabla^2)^2\varphi \tag{3}$$

is the chemical potential difference between the two components, Γ is a mobility coefficient, and the Laplacian on the r.h.s. guarantees the conservation of φ. The velocity $\mathbf{u}$ is the local fluid velocity. It obeys the Navier–Stokes equation which, in the incompressibility limit $\boldsymbol{\nabla}\cdot\mathbf{u} = 0$, reads as

$$\partial_t u_\alpha + \mathbf{u}\cdot\boldsymbol{\nabla}u_\alpha = -\frac{1}{n}\partial_\beta P^{th}_{\alpha\beta} + \nu\nabla^2 u_\alpha, \tag{4}$$

where ν is the kinematic viscosity. $P^{th}_{\alpha\beta}$ is the thermodynamic pressure tensor

$$P^{th}_{\alpha\beta} = \left\{n\frac{\delta F}{\delta n} + \varphi\frac{\delta F}{\delta\varphi} - f(n,\varphi)\right\}\delta_{\alpha\beta} + D_{\alpha\beta}(\varphi), \tag{5}$$

where $f(n,\varphi)$ is the free-energy density and a symmetric tensor $D_{\alpha\beta}(\varphi)$ has to be added to ensure that the condition of mechanical equilibrium $\partial_\alpha P^{th}_{\alpha\beta} = 0$ is satisfied [8]. The complete expression of

the pressure tensor is [3]

$$P^{th}_{\alpha\beta} = \left\{\frac{1}{3}n + \frac{a}{2}\varphi^2 + \frac{3}{4}b\varphi^4 - \kappa\left[\varphi(\nabla^2\varphi) + \frac{1}{2}(\nabla\varphi)^2\right] + d\left[\varphi(\nabla^2)^2\varphi + \frac{1}{2}(\nabla^2\varphi)^2 + \partial_\gamma\varphi\partial_\gamma(\nabla^2\varphi)\right]\right\}\delta_{\alpha\beta} + \kappa\partial_\alpha\varphi\partial_\beta\varphi - d[\partial_\alpha\varphi\partial_\beta(\nabla^2\varphi) + \partial_\beta\varphi\partial_\alpha(\nabla^2\varphi)]. \quad (6)$$

Eqs. (2)–(4) are numerically solved using a mixed approach. We use a finite difference scheme for Eq. (2) and the LBM for Eq. (4). Such an approach has been already adopted in the case of thermal lattice Boltzmann models for a single fluid [9] and for multiphase flows [10]. In that case it is the temperature equation to be solved by finite differences. The reasons that justify our approach are dictated by the possibility of avoiding the spurious terms in the convection–diffusion equation (2) which come into play when standard LBM for binary mixtures is used [6], though LBM may realize boundary conditions (BC) easily and give better numerical stability. Moreover, the amount of required memory can be dramatically decreased so that larger systems can be simulated and the simulation of quite big systems in three dimension is finally possible. For the two-dimensional model on a square lattice with nine velocities that we use in the present study, we can use just $\frac{1}{9}$ of the RAM that we would have used by using LBM to solve Eq. (2).

A set of distribution functions $f_i(\mathbf{r}, t)$ is defined on each lattice site $\mathbf{r}$ at each time t. Each function is associated to a lattice speed vector $\mathbf{e}_i$ with $e_i/c = (\pm1, 0), (0, \pm1), (\pm1, \pm1), (0, 0)$, where $c = \Delta x/\Delta t$, Δt is the time step and Δx is the lattice constant.

They evolve according to a single relaxation-time Boltzmann equation [4,11]:

$$f_i(\mathbf{r} + \mathbf{e}_i\Delta t, t + \Delta t) - f_i(\mathbf{r}, t) = -\frac{1}{\tau}[f_i(\mathbf{r}, t) - f_i^{eq}(\mathbf{r}, t)], \quad i = 0, \ldots, 8, \quad (7)$$

where τ is a relaxation parameter and $f_i^{eq}(\mathbf{r}, t)$ are local equilibrium distribution functions. The distribution functions are related to the total density n and to the fluid momentum $n\mathbf{u}$ through

$$n = \sum_i f_i, \quad \mathbf{u} = \frac{1}{n}\sum_i f_i\mathbf{e}_i. \quad (8)$$

These quantities are locally conserved in any collision process and, therefore, we require that the local equilibrium distribution functions fulfil the equations $\sum_i f_i^{eq} = n$ and $\sum_i f_i^{eq}\mathbf{e}_i = n\mathbf{u}$. Following Ref. [6], the higher moments of the local equilibrium distribution functions are defined so that the Navier–Stokes equation can be obtained and the equilibrium thermodynamic properties of the system can be controlled: $\sum_i f_i^{eq} e_{i\alpha}e_{i\beta} = c^2P^{th}_{\alpha\beta} + nu_\alpha u_\beta$. The local equilibrium distribution functions can be expressed as an expansion at the second order in the velocity $\mathbf{u}$ [6]. The expression of the coefficients of the equilibrium distribution functions can be found in Ref. [12].

The above described lattice Boltzmann scheme simulates at second order in Δt the continuity and the incompressible Navier–Stokes equations (4) with the kinematic viscosity ν given by $\nu = \Delta t(c^2/3)(\tau - \frac{1}{2})$. It appears that the relaxation parameter τ can be used to tune independently viscosity.

Eq. (2) is numerically integrated by using an explicit Euler scheme on a square lattice with spacing Δx, the same as for LBM. The spatial derivatives are approximated by discrete expressions which are second order in Δx. The time step is $\Delta t' = \Delta t/m$ with $m = 2$. This choice was motivated by the observation of a better numerical stability of the code. For the problem considered in this paper we used the following BC. We assume that the shear is applied in the x direction so we assume periodic BC along this direction. In the y direction the BC are enforced in the following way. In order to shear the system, we do not enforce from the outside a desired velocity profile but we place walls at top and bottom rows of the lattice moving them at a constant velocity along the x direction avoiding slip velocity [13]. The velocity profile obtained from Eq. (8) goes inside the convection–diffusion equation (2). For the order parameter φ we adopt Lees-Edwards BC along the y direction [14]. This means that $\varphi(x, 0) = \varphi(x + (u_t - u_b)\Delta t', L)$, where L is the size of the lattice and u_t and u_b are the velocities of the top and bottom walls, respectively. This guarantees that φ is sheared also in virtual lattice nodes beyond the walls which need to be taken into account in order to compute the spatial

derivatives of φ at walls. This choice ensures the better stability at walls. The algorithm works in the following way:

(1) Initialize variables f_i (such that $n = 1$) and φ (randomly taken in the range $[-0.1, 0.1]$).
(2) Compute the quantities μ and $\mathbf{u}$ from Eqs. (3) and (8), respectively.
(3) Iterate Eq. (2) for m time steps $\Delta t'$.
(4) Compute the pressure tensor $P^{th}_{\alpha\beta}$ from Eq. (6) by using φ and n.
(5) Compute f_i^{eq}.
(6) Iterate Eq. (7) for one time step Δt.
(7) Go to (2).

3. Numerical results and discussion

The numerical results here presented were obtained on a lattice with size $L = 1024$. The following parameters were used: $a = -b = -2 \times 10^{-4}$, $\kappa = -6 \times 10^{-4}$, $d = 7.6 \times 10^{-4}$, $\Gamma = 25$, $\tau = 3$, $\Delta x = 1$, and $\Delta t = 0.2$. The choice $|a| = b$ is such that the minimum of the polynomial terms in the free energy (1) is in $\varphi = \pm 1$. For the selected parameters the equilibrium state is lamellar. The width of a lamellar is $\lambda/2 = \pi/q = 5$ in units of lattice spacings. The velocity of walls was set to $u_t = -u_b = \dot{\gamma}L/2$. We used the values $\dot{\gamma} = 10^{-4}, 10^{-3}$. The kinematic viscosity is $v = 4.16$. The system was initialized in a disordered state with $\varphi = \varepsilon$ where ε is a random number uniformly distributed in the range $[-0.1, 0.1]$ and $f_i = 1/9$, $i = 0, 1, \ldots, 8$, such that $n = 1$.

At the larger values of shear rate considered, the system reaches almost completely ordered states with lamellae parallel to the walls. This can be observed in the left panel of Fig. 1 for the case $\dot{\gamma} = 10^{-3}$ where only few local defects are still present at the time of the figure. The situation is different from the case without applied flow [15], where the late time dynamics was shown to be characterized by the presence of extended defects consisting of grain boundaries between domains of differently oriented lamellae. Order was never reached on the scale of the whole system simulated and the characterization of the asymptotic dynamics of lamellar phases is still an open problem.

The presence of imposed flow favours the ordering of lamellae, well aligned on the whole horizontal size of the system, first close to the walls and later in the inner part of the system. Lamellar order has been observed to develop towards the central part of the system together with the formation of the velocity profile of planar

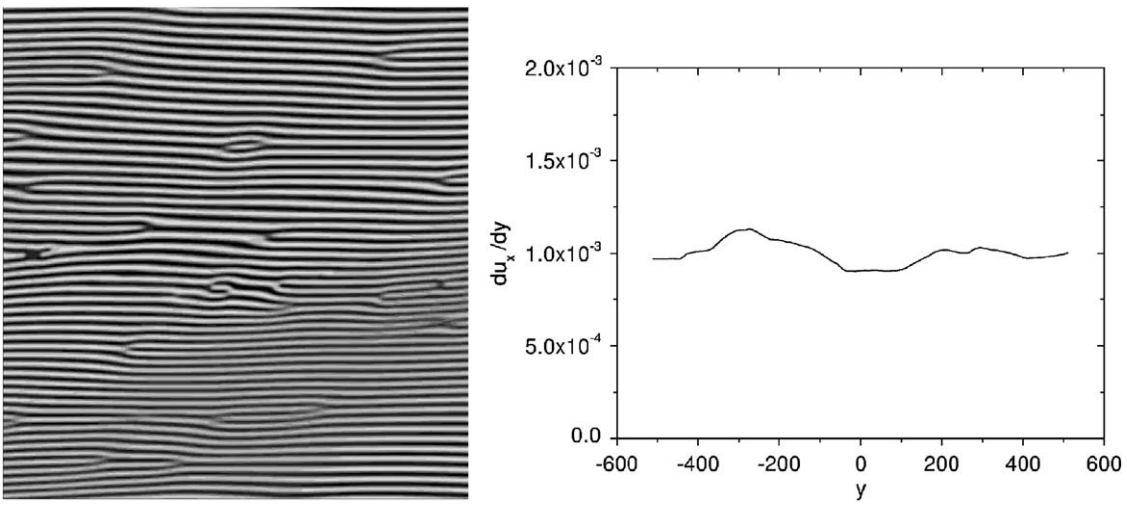

Fig. 1. Left panel: configuration of the order parameter φ in the case $\dot{\gamma} = 10^{-3}$ at time $t = 26,400$ on the central portion 512×512 of the whole lattice. Right panel: averaged shear rate across the system in the same case at the same time.

shear flow. In the right panel of Fig. 1, with order almost developed in the whole system, the average shear rate is close to the imposed value; fluctuations around the linear velocity profile are generally observed to decrease with time.

At lower shear rates, like the case of Fig. 2 at time $t = 40,600$, the system shows the phenomenon of shear banding discussed in the introduction. Close to the walls lamellae are still well aligned but in the middle of the system order is not observed even at the latest times of simulations. Indeed, lamellae are not aligned with the flow showing a finite tilt angle. Moreover, there is a plenty of topological defects which characterizes the morphological pattern.

At very long times the lamellar phase has been observed to coexist with a more viscous middle phase consisting of tilted domains, pieces of bended lamellae and droplets. We have found the number of droplets to increase with time. Since the averaged order parameter has to remain zero due to the conservation law, we expect that the middle phase can be described as a mixture of A-droplets in B-matrix and B-droplets in A-matrix. This phase does not exist in equilibrium and is induced by the flow. This behaviour has been also observed in simulations with other values of $\dot{\gamma}$ less than 5×10^{-4}.

The shear rate profile at time $t = 40,600$ is also shown in Fig. 2. We stress that the shear rate profile has been observed to remain stationary from $t \sim 30,000$ until the latest time $t = 10^5$ of the simulations. We see that the profile is banded with the value close to the walls and the value in the inner part of the system, respectively, greater and smaller than the imposed value. This is typical of shear banding phenomena. The region with low shear rate corresponds to the extension of the SIS phase ($\sim$200 lattice spacing). We see that there is an interfacial region between the two regions with different shear rates. The width of this region is quite extended ($\sim$150 lattice spacing) confirming the relevance of diffusive terms introduced in constitutive models by Olmsted et al. [16]. We also observe that the velocity in the central band is very close to zero. This is typical of yield stress phenomena where "pasty" phases do not flow also at finite values of stress. Shear banding in yield stress fluids has been found experimentally in systems with lamellar order [17].

A more complete discussion of the kinetics of shear banding for lamellar systems on the basis of our results will be presented elsewhere. The main purpose of this paper has been to show that numerical methods based on mesoscopic models like that of Section 2 can be very effective for describing complex fluids dynamics. In particular the LBM approach combined with finite difference schemes for diffusion–convection equation allows a detailed description of defects dynamics and local velocity also in very complex phenomena like shear banding. This is not possible in methods based on constitutive equations where only the behaviour of stress is considered without taking into considerations the evolution of local structures.

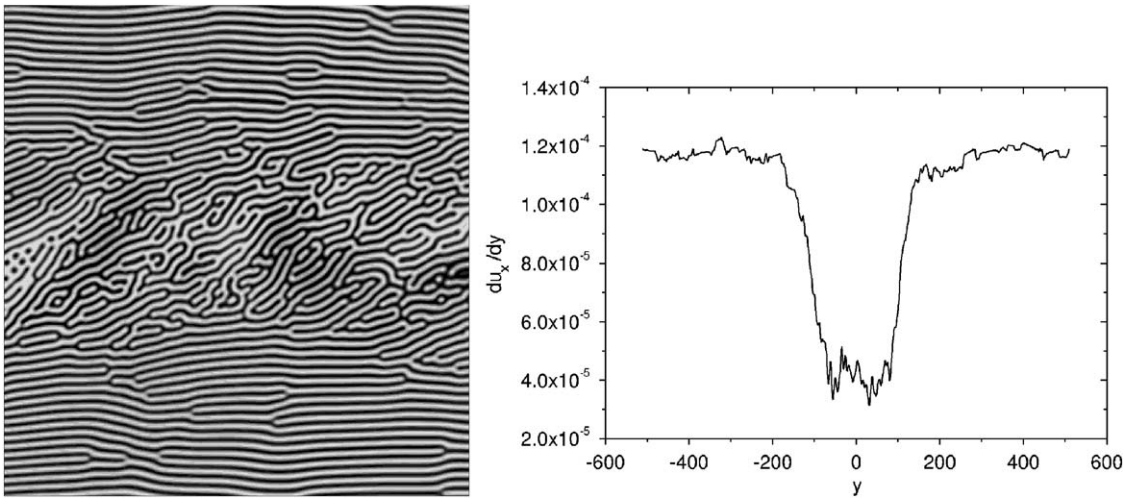

Fig. 2. Left panel: configuration of the order parameter φ in the case $\dot{\gamma} = 10^{-4}$ at time $t = 40,600$ on the central portion 512×512 of the whole lattice. Right panel: averaged shear rate across the system in the same case at the same time.

Acknowledgements

This work has been partially supported by MIUR (PRIN-2002).

References

[1] R.G. Larson, The Structure and Rheology of Complex Fluids, Oxford University Press, New York, 1998.
[2] P.D. Olmsted, Europhys. Lett. 48 (1999) 339.
[3] G. Gonnella, E. Orlandini, J.M. Yeomans, Phys. Rev. Lett. 78 (1997) 1695;
G. Gonnella, E. Orlandini, J.M. Yeomans, Phys. Rev. E 58 (1998) 480.
[4] S. Succi, The Lattice Boltzmann Equation, Oxford University Press, New York, 2001.
[5] T.M. Rogers, K.R. Elder, R.C. Desai, Phys. Rev. B 37 (1988) 9638.
[6] E. Orlandini, M.R. Swift, J.M. Yeomans, Europhys. Lett. 32 (1995) 463;
M.R. Swift, et al., Phys. Rev. E 54 (1996) 5041.
[7] S.A. Brazovskii, Sov. Phys. JETP 41 (1975) 85.
[8] R. Evans, Adv. Phys. 28 (1979) 143.
[9] O. Filippova, D. Hänel, Int. J. Mod. Phys. C 9 (1998) 1439;
O. Filippova, D. Hänel, J. Comput. Phys. 158 (2000) 139;
P. Lallemand, L.S. Luo, Phys. Rev. E 68 (2003) 036706.
[10] R. Zhang, H. Chen, Phys. Rev. E 67 (2003) 066711.
[11] P. Bhatnagar, E.P. Gross, M.K. Krook, Phys. Rev. 94 (1954) 511.
[12] A. Xu, G. Gonnella, A. Lamura, Physica A 331 (2004) 10.
[13] A. Lamura, G. Gonnella, Physica A 294 (2001) 295.
[14] A.W. Lees, S.F. Edwards, J. Phys. C 5 (1972) 1921.
[15] G. Amati, G. Gonnella, A. Lamura, F. Massaioli, A. Xu, Int. J. Mod. Phys. C, accepted for publication.
[16] C.-Y. David Lu, P.D. Olmsted, R.C. Ball, Phys. Rev. Lett. 84 (2000) 642.
[17] G. Picard, A. Ajdari, L. Bocquet, F. Lequeux, Phys. Rev. E 66 (2002) 051501.